

1 Smoothed factor analysis for identifying trends in multivariate time
2 series

3 Eric J. Ward¹

4 ¹Conservation Biology Division, Northwest Fisheries Science Center, National Marine Fisheries Service,
5 National Oceanic and Atmospheric Administration, 2725 Montlake Blvd E, Seattle WA, 98112, USA

6

Abstract

Ecological processes are rarely directly observable, and for many systems, variance parameters are unknown and must be estimated from data. State space models have become widely used in the environmental sciences, particularly for time series data, because of their ability to simultaneously estimate multiple sources of variation (process or natural variability, and variance attributed to observations, associated with measurement and sampling errors). A common state space approach for using multivariate time series to identify underlying signals from corrupted data is dynamic factor analysis. The conventional dynamic factor model is flexible in that unseen processes are modeled as random walks. While this may be suitable for some situations, random walks may be overly complex for other cases. In this paper, we introduce a new class of dynamic factor models, where latent processes are modeled as smooth functions. We highlight two alternatives to the random walk approach, using basis splines and Gaussian predictive process models. These models are applied to two long term datasets from the west coast of the United States: (1) a 35 year dataset juvenile rockfishes from the west coast of the United States, and (2) a 39 year dataset of fisheries catches. We compare the out of sample predictive accuracy of our new approaches to conventional models with cross-validation, and find that for both applications, the smooth trend models result in models with higher predictive accuracy.

Key words

Dynamic factor analysis, smooth spline, B-spline, Gaussian process, Bayesian modeling, Stan

24 Introduction

25 Ecological data can be characterized by multiple sources of variability, including stochastic natural variation,
26 and errors associated with data collection (observation, sampling, and measurement errors). Disentangling
27 these sources of variability is often challenging, and necessitates the use of complex statistical methods, such
28 as state space models. These approaches have become ubiquitous in ecology, particularly for time series
29 data (Auger-Méthé et al. 2020) – in part because these models allow researchers to make inferences about
30 ecological processes that aren’t directly observable via corrupted observations. Applications of these models
31 include estimating population change over time (Clark and Bjørnstad 2004), movement dynamics (Patterson
32 et al. 2008), and understanding spatiotemporal variation (Anderson and Ward 2019).

33 Estimating multiple sources of variation in state space models is numerically complex, and can be
34 constrained explicitly or implicitly in ecological models via model assumptions. For example, discrete time
35 state-space models of population trajectories generally assume latent population size can be approximated by
36 an autoregressive process in log-space $x_{t+1} = f(x_t) + \epsilon_t$, where $x_t = \log(n_t)$ and ϵ_t are normally distributed
37 process deviations representing stochastic variability of the natural system (Dennis et al. 2006). The autore-
38 gressive assumption is critical here; without such a constraint, the variance of the stochastic noise ϵ_t is not
39 estimable in the presence of an observation or data model. Separating out these sources of variability is crit-
40 ical for being able to generate unbiased estimates of population trends, or density dependence (Knappe 2008).
41 If inference is not dependent on parameters of ecological interest (e.g. growth rates, density dependence), a
42 wide range of alternative semi-parametric approaches exist that can be used to model the trajectory of x_t ,
43 including generalized additive models (GAMs, (Wood 2011)) and Gaussian process models (Roberts et al.
44 2013). Because these models are not autoregressive with discrete time steps, the flexibility or ‘wiggleness’ of
45 the model can be adjusted as part of the model fitting. In addition to their flexibility, these semi-parametric
46 models of may be better suited for situations when data are patchily distributed in time or unequally spaced,
47 making estimation of process and observation errors more difficult.

48 Challenges posed by univariate time series models also apply to multivariate time series models, though
49 one additional complexity introduced by the multivariate setting is that the number of latent time series
50 may be variable, $k = 1, \dots, m$, where m is the number of time series observed. At one extreme, $k = m$,
51 and each time series can be thought of as corresponding to a unique latent state. Motivating questions in
52 analyzing these kinds of data include estimating correlated latent processes or trends, or estimating effects
53 of environmental covariates on sub-populations (Hovel et al. 2016). At the other extreme, $k = 1$, where
54 each time series can be thought of as replicates or multiple measurements of the same trajectory of states,

with optional offsets or coefficients included for each time series (offsets allowing for differing detectability). Applications focused on estimating a single trend from multivariate data include the development of ecological indicators. Models with intermediate numbers of latent states $1 < k < m$ require mapping of time series to latent trends. These may be specified a priori (Ward et al. 2010) or estimated within the modeling framework using dimension reduction techniques.

Many statistical approaches have been proposed in recent years for clustering or estimating common signals in multivariate time series (Liao 2005). Examples include clustering based on similarities among time series features (Sardá-Espinosa 2019), identifying common patterns in the frequency domain (Holan and Ravishanker 2018), and clustering based on neural networks (Cherif et al. 2011). Application of these methods to ecological data has been limited, however, in part because many of these approaches identify clusters from raw data and don't explicitly account for observation error. An alternative approach that has been used in ecology to map collections of multivariate time series to latent states, while accounting for observation error, is dynamic factor analysis (DFA) (Zuur et al. 2003b, 2003a). DFA is an extension of factor analysis for time series data, and estimates a small number of unobserved processes, referred to as trends, that can describe observed data. Mapping time series to trends is done via estimated factor loadings – these allow each time series to be modeled as a mixture of the estimated latent trends, rather than assigning each time series to a single trend.

To date, applications of DFA models in ecology and other fields have assumed that underlying trends are modeled as a random walk, $x_{t+1} = x_t + \epsilon_t$. The objective of this analysis is to introduce a new class of DFA models for multivariate time series. Just as the univariate autoregressive model described above can be approximated with smooth functions, DFA models may be extended to use smooth functions in lieu of autoregressive processes. Recent work has highlighted the application of hierarchical GAMs for multiple data sources (Pedersen et al. 2019). These approaches are flexible and likely to provide similar inference to DFA for single latent trend, however these methods have not been extended to include more than one process. We illustrate two options for modeling smooth functions for latent trends: basis splines ('B-splines') and Gaussian process models. Both approaches are compared to conventional autoregressive DFA models for two datasets on marine fishes from the west coast of the USA. All data and code are for replicating our analysis are on Github, and in our existing R package 'bayesdfa' (Ward et al. 2019).

Methods

Dynamic Factor Model

The basic DFA model can be written as a multivariate state space model, consisting of a latent process model and observation or data model. In its simplest form, the process model is expressed as a random walk, $\mathbf{x}_{t+1} = \mathbf{x}_t + \mathbf{w}_t$, where $\mathbf{w}_t \sim MVN(0, \mathbf{Q})$. For identifiability constraints (Zuur et al. 2003b, Holmes et al. 2012), the covariance matrix \mathbf{Q} is generally constrained to be an identity matrix. Additional features may be incorporated into the process model, including autoregressive or moving average coefficients, covariates, or deviations that are more extreme than that of the normal distribution (Ward et al. 2019). The observation model in a DFA is expressed as a linear combination of trends \mathbf{x}_t and matrix of loadings coefficients \mathbf{Z} , $\mathbf{y}_t = \mathbf{Z}\mathbf{x}_t + \mathbf{B}\mathbf{d}_t + \mathbf{e}_t$. In addition to the trends and loadings, time varying covariates \mathbf{d}_t may be optionally included and linked to the observations through estimated coefficients \mathbf{B} . The vector \mathbf{e}_t represents residual observation error. These typically are modeled as a diagonal matrix, $\mathbf{e}_t \sim MVN(0, \mathbf{R})$ but off-diagonal elements may be estimated (Holmes et al. 2020). Further details of the Bayesian implementation of the DFA model and extensions are provided in (Ward et al. 2019).

Modeling trends as Gaussian processes

Conventional DFA models with trends modeled as random walks are flexible, but for some datasets these models may be too complex. As a first alternative approach to the random walk model, we treat the trends as a Gaussian process model. A discrete time Gaussian process model of trends treats the vector representing each trend as a stochastic process, where \mathbf{x}_k is drawn from a multivariate normal distribution. As data in a DFA are generally standardized, we can assume the mean of each trend to be 0, and all inference about the Gaussian process occurs the covariance matrix, $\mathbf{x}_k \sim MVN(0, \Sigma)$. Rather than estimate each element of Σ independently, smooth covariance functions or ‘kernels’ are chosen to represent the covariance between points in time (typical choices include the exponential, Gaussian, and Matern functions). For the purpose of our DFA modeling, we adopt a Gaussian kernel. With this kernel, the covariance between points i and j at times t_i and t_j on trend k can be expressed as $cov(x_{i,k}, x_{j,k}) = \sigma_k^2 \exp\left(\frac{-(t_i - t_j)^2}{2\theta_k^2}\right)$, where σ_k controls the magnitude of variation, and θ_k controls how smoothly correlation decreases as time points become further apart. We allow each trend to have its own covariance parameters, allowing each to have differing degrees of smoothness. Because of potential computation issues in high dimensionality problems such as spatial models (Latimer et al. 2009, Anderson and Ward 2019), we also allow this Gaussian process model to be expressed as a Gaussian predictive process model. The difference between the predictive process approach

and the full Gaussian process model is that instead of modeling the \mathbf{x}_t themselves as random variables, random variables are modeled at a subset of locations \mathbf{x}_k^* (these locations are referred to as ‘knots’) and projected to the locations of the data \mathbf{x}_k . If we assume $\mathbf{x}_k^* \sim MVN(0, \Sigma^*)$, then this projection can be done as $x_k = \Sigma'_{k,k^*} \Sigma^{*-1} x_{k^*}^*$, where the matrix Σ'_{k,k^*} is the transpose of the matrix describing the covariance between x_k and $x_{k^*}^*$. The location of k^* can be spaced equally or depend on data; for the purposes of our DFA modeling, we assume that the k^* are equally spaced within each time series (with the endpoints also acting as knots).

Modeling trends as splines

As a second alternative model of latent trends in a DFA, we use a series of smoothing functions, known as basis splines (‘B-splines’). These models can be thought of as a special case of Gaussian process models (Kimeldorf and Wahba 1970), and offer flexibility similar to the more familiar generalized additive models (Wood 2011). B-splines are represented as a series of piecewise polynomial functions, where higher order polynomials result in more flexible curves (Hastie 1992). A common choice of the order of these polynomials is a cubic or 3rd degree, and will be the focus of our implementation for DFA models. An additional input to B-splines is the locations of the control points between polynomial segments – more control points translate into a more flexible function, but also one with more parameters to estimate. Similar to Gaussian process models, the locations of these control points are referred to as knots, and are generally selected within the temporal domain of the data. For our applications to DFA, we assume knots to be uniformly distributed over the time series. Uniform knot vectors may be appropriate for data collected at regular intervals, but for observations more patchily distributed in time, a non-uniform distribution may be warranted.

Mathematically, modeling the trends in a DFA with B-splines can be expressed as a linear combination of the matrix describing the B-splines \mathbf{B} and estimated coefficients \mathbf{a} , $\mathbf{x}_k = \mathbf{a}\mathbf{B}$. The matrix \mathbf{B} describes the B-splines, and can be viewed as a matrix of weights that is generated from the raw data prior to estimation. In the DFA setting, \mathbf{B} is shared across trends, but for trend-specific variability, we allow the coefficients \mathbf{a} to have a variance parameter unique to each trend, $\mathbf{a}_k \sim Normal(0, \sigma_k)$.

Application: 1-trend models of larval fish dynamics

As a first application of smooth factor analysis models, we apply DFA to a long term time series of larval fishes collected in Southern California (USA). The California Cooperative Oceanic Fisheries Investigations (CalCOFI) survey has been collecting physical and biological samples since 1949, to monitor annual, seasonal,

and spatial changes to the California Current Ecosystem (Bograd et al. 2003). The CalCOFI data has been incorporated into models used to assess population status (MacCall 2003), and numerous publications have used time series of larval fishes from the CalCOFI survey as indicators of ecosystem state (Mcclatchie et al. 2008). These types of motivating questions also present an opportunity to apply DFA with both conventional and smoothed trends to summarize ecosystem state indices. For this application, we focus on the dynamics of three species of juvenile rockfishes: Aurora rockfish (*Sebastes aurora*), Shortbelly rockfish (*S. jordani*), and Bocaccio rockfish (*S. paucispinis*). For the purposes of this analysis, we restrict the time series to data collected since 1985, when sampling has been consistent in space and time (Moser et al. 2001). Though CalCOFI cruises are done throughout the year, we are primarily interested in estimating interannual trends, and thus restrict our analysis to considering spring cruises from 1-April to 22-May when densities of most rockfish species are highest (Mosek et al. 2000). All data were retrieved using R software (R Core Team 2020) and the rerddap package (Chamberlain 2020).

With only three time series, we focus on identifying models estimating a single shared trend and single observation error variance, shared across species. Other types of models, including hierarchical GAMs (Pedersen et al. 2019) or models allowing estimated offsets may also be useful in this type of application. Where the DFA model differs is that unlike models with random intercepts or additive offset terms, the DFA factor loadings \mathbf{Z} are multiplicative and may be close to zero. These cases may arise when a particular time series has a low signal to noise ratio, or if there is low correspondence with the latent trends estimated among all other time series. In addition to estimating a conventional 1-trend DFA model with a latent autoregressive process, we evaluate 1-trend B-spline and GP models. Because we have no a priori hypotheses about the complexity of these smoothed factor models, we evaluated 5 models for each, using 6, 12, 18, 24, and 30 equally spaced knots.

Application: 2-trend models of commercial fisheries catches

As a slightly more complex example of the smooth factor analysis model, we examine the performance of 2-trend models, using a dataset of commercial fisheries catches (landings) from the west coast of the USA. This dataset consists of landings by dominant species, and is reported annually to the Pacific Fishery Management Council (PFMC 2020). This dataset consists of 13 species or groups reported over a 39 year period (1981 – 2019). Landings on the west coast are dominated by Pacific hake (also Pacific whiting, *Merluccius productus*), but also include substantial catches of rockfishes (*Sebastes spp.*) and flatfishes (e.g. Dover sole, *Solea solea*). Over the course of the last 4 decades, these species have experienced variability associated with population dynamics and the environment, but the patterns of landings also reflects a dynamic fisheries management

process. Examples of changes include temporarily closing areas to fishing to protect species of conservation concern, and implementing catch share programs. These processes, combined with environmental conditions that have been positive for many species have resulted in many increasing populations (Warlick et al. 2018). Given these various management and ecological changes, it is important to summarize patterns of landings, and identify common trends as indicators for management and ecosystem status (Harvey et al. 2018).

As with our previous example, we compared conventional DFA models to those modeling the trends with smooth functions. Preliminary model fitting suggested that 2-trend models were more supported by the data, and thus will be the focus of our analysis. In addition to modeling the 2-trend model with conventional DFA, we evaluated B-spline and Gaussian process models with 6 to 30 equally spaced knots. All models included a single shared observation error variance, shared across time series.

Estimation and model selection

We developed our DFA model in a Bayesian framework, using Stan and the package rstan (Stan Development Team 2016), which implements Markov chain Monte Carlo (MCMC) using the No-U Turn Sampling (NUTS) algorithm (Hoffman and Gelman 2014, Carpenter et al. 2017). For each model considered, we ran 3 parallel MCMC chains for 3000 iterations each, discarding the first 50% of the samples. Convergence diagnostics were assessed using summary statistics (R-hat, (Gelman and Rubin 1992)). Previous approaches have used the Leave One Out Information Criterion (LOOIC) as a model selection tool (Vehtari et al. 2017, 2020). Preliminary model checks using LOOIC for the models included in our analysis indicated that many models had 1-4 data points that had high Pareto-k statistics (possibly because of model-misspecification or model flexibility; Vehtari et al. (2017)). As a slower but potentially more robust model selection approach, we implemented k-fold cross validation. There are many possible ways to assign ‘folds’ in cross-validation, and because of our focus on the temporal aspect of these DFA models, we assigned each year of data to a unique fold. Implementing these models using cross validation results in increased computational time; instead of fitting each model to a dataset once, a single model is re-fit to a dataset for as many years as there are data (35 years for our application to CalCOFI data; 39 years for our application to commercial landings data).

As a measure of predictive accuracy, we used the cross-validation results for each of the models in our applications to calculate the expected log pointwise predictive density (ELPD). In the context of our cross-validation with each time step as a fold, the formula for ELPD is $ELPD = \sum_{k=1}^T \log(p(\mathbf{y}_k | \mathbf{y}_{-k}))$, where k indexes time steps $1, 2, \dots, T$ and $p(\mathbf{y}_k | \mathbf{y}_{-k}) = \int p(\mathbf{y}_k | \theta) p(\theta | \mathbf{y}_{-k}) d\theta$ (Vehtari et al. 2017). Code for many classes of Bayesian models is available in the loo package (Vehtari et al. 2020), and extensions for

DFA models are made available in our bayesdfa package (Ward et al. 2019).

Results

For our application of smooth dynamic factor models to the CalCOFI juvenile rockfish dataset, we found that the B-spline trend model with 6 knots had slightly better (higher) ELPD values than alternatives (Table 1). Aside from the conventional random walk DFA model which resulted in the lowest ELPD value, many models had similar ELPD values, indicating similar predictive ability. This can also be confirmed by examining predictions, where many models appeared to capture the dynamics of the three *Sebastes* time series well (Fig. 1). All three species were estimated to have positive loadings on the estimated trend, with shortbelly rockfishes having the highest loading (0.81, 95% posterior interval = -0.84-2.66) followed by aurora (0.5, 95% posterior interval = 0.03-1.62) and bocaccio rockfishes with the weakest loadings (0.23, 95% posterior interval = -0.5-1.15). Though the model with 6 knots was found to have the highest predictive accuracy, the simplicity of this model affected the ability to capture the most recent variability in the time series between 2015-2019, when juvenile rockfish densities were among the highest ever observed (Fig 1).

When smooth trend B-spline and Gaussian predictive process models are applied to commercial fisheries landings data, the model with the highest ELPD was the B-spline model with 24 knots. Across all models, those that modeled trends as B-splines had higher predictive accuracy than those that modeled trends as Gaussian processes or random walks (Table 2). All models considered for this dataset included 2 latent trends. The first trend exhibited nearly linear change from 1981 - 2001 and was relatively stationary from 2001 - 2019 (Fig. 2). The second trend represented change from the early 1990s, with the strongest change occurring 2010 - present. Estimates of the loadings from the model with highest ELPD indicated most species or species groups loaded negatively on trend 1, with the exception of Pacific whiting (Fig. 3). Trend 2 from this model appears to contrast species with relatively stationary catches before declining in 2010 (e.g. Arrowtooth flounder, *Atheresthes stomas*) versus Petrale sole (*Eopsetta jordani*) - one of the only non-whiting species that has experienced positive catches since 2010. Predictions across all models appeared to characterize the trends of most species - though none of the approaches were able to capture the variability in Pacific whiting catches since 2000 (Fig. 4).

Discussion

We found that when compared to conventional DFA with trends as random walks, modeling trends as smooth functions resulted in models with higher predictive ability for out of sample cross-validation. Both

applications in our analysis highlighted that models with trends as B-splines received the highest support, and that these models had better predictive ability than Gaussian predictive process models. Several important caveats in our comparisons are that the model predictions and resulting ELPD estimates are conditioned on the location and number of knots. For models with missing data, or datasets with unevenly distributed replicate samples, it may be important to consider non-uniform knot vectors.

Add a few sentences about case studies etc

There are several important differences between the conventional random walk DFA model, and the smooth trend models developed here. In the random walk model, observations

Because of their flexibility, applications of LOOIC or related model selection to DFA models may result in poor diagnostics. As an alternative, we implemented cross-validation in two applications to identify the model with the highest predictive accuracy. In each case, we implemented k-fold cross validation with each year of the time series held out in turn and predicted from the remaining data. Our first application of these methods to the CalCOFI juvenile rockfish dataset highlighted that models with high predictive accuracy across the full time series may not be the best for capturing variation in particular periods of interest. Between 2015 - 2019 for example, the three rockfish species in our case study experienced a pulse that was not captured by simpler smooth models (Fig. 1) - despite those models having higher predictive accuracy across the time series. Several alternative approaches to cross validation may be useful if predictions in some years are more important than others. For example, the analysis of CalCOFI data could be repeated, but the ELPD could be calculated using only the last decade as test data. A second approach would be to implement leave-future-out cross-validation, which differs from our approach in that data points are only used to predict future years, not historical values (Bürkner et al. 2020). While none of the models included in our analysis included covariates, the cross-validation approaches described here can be extended identify predictor variables (such as environmental drives) that result in increased predictive accuracy.

Acknowledgments

Tables

Table 1. Expected log posterior density (ELPD, with standard errors) for each of the models applied to our cases studies (CalCOFI time series of juvenile rockfishes, and the time series of commercial groundfish landings from the west coast of the USA). The B-spline models are generated with basis splines, and the Gaussian predictive process models are generated using a Gaussian covariance function. For each model, knots (or locations of control points) are assumed to be uniformly spaced over the time series.

Trend.model	Knots	CalCOFI.ELPD	CalCOFI.SE	Landings.ELPD	Landings.SE
Random walk	NA	55.34	12.55	-26088.92	298.83
B-spline	6	93.02	12.38	-25605.43	328.90
B-spline	12	92.64	12.57	-25488.23	312.53
B-spline	18	92.31	12.72	-25512.17	300.25
B-spline	24	92.94	12.31	-25438.14	332.20
B-spline	30	92.92	12.53	-25494.47	309.56
Gaussian process	6	88.16	13.87	-26308.22	345.78
Gaussian process	12	88.84	13.47	-26097.53	324.82
Gaussian process	18	88.95	13.40	-26282.30	354.38
Gaussian process	24	88.42	13.76	-25932.45	320.96
Gaussian process	30	88.36	13.67	-26164.90	329.55

Figure Captions

Figure 1. Standardized densities of juvenile shortbelly rockfish collected in the CalCOFI survey, and estimates of latent trends for three candidate models, representing a range of flexibility in splines compared to the conventional random walk. A B-spline model with 6 knots had slightly higher ELPD values than other smooth trend models (such as the more coarse 12 knot model) and the conventional DFA (random walk). The posterior mean from each model is shown as a solid black line, and 95% credible intervals are shown in the grey region.

Figure 2. Estimated trends from the 2-trend DFA model applied to commercial groundfish landings off the west coast of the United States. The model results with lowest LOOIC is shown, a model that allows trends to be approximated with B-splines (6 knots). The posterior mean for each trend is shown, with ribbons representing 95% credible intervals.

Figure 3. Estimated loadings for each species or group from a 2-trend DFA model with latent trends modeled as B-splines. The posterior mean for each species is shown as a point, with lines representing 95% credible intervals.

Figure 4. Estimated landings for 2 species included in our analysis, with contrasting trends (lingcod, Pacific whiting). Posterior means and 95% credible intervals (ribbons) for three candidate models are shown: b-spline trend models with 6 and 18 knots, respectively, and a random walk model representing the conventional DFA model.

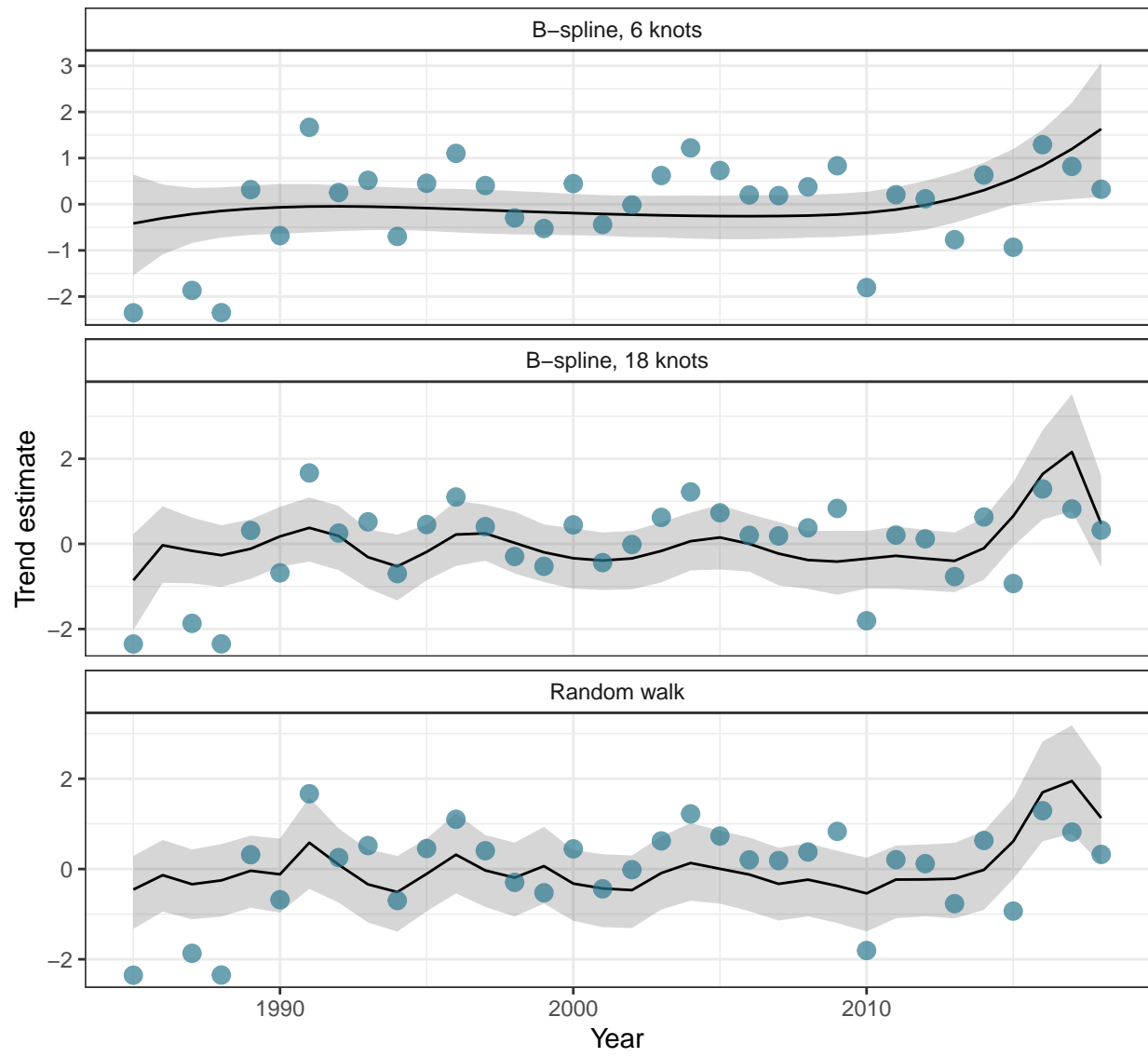


Figure 1: Figure 01

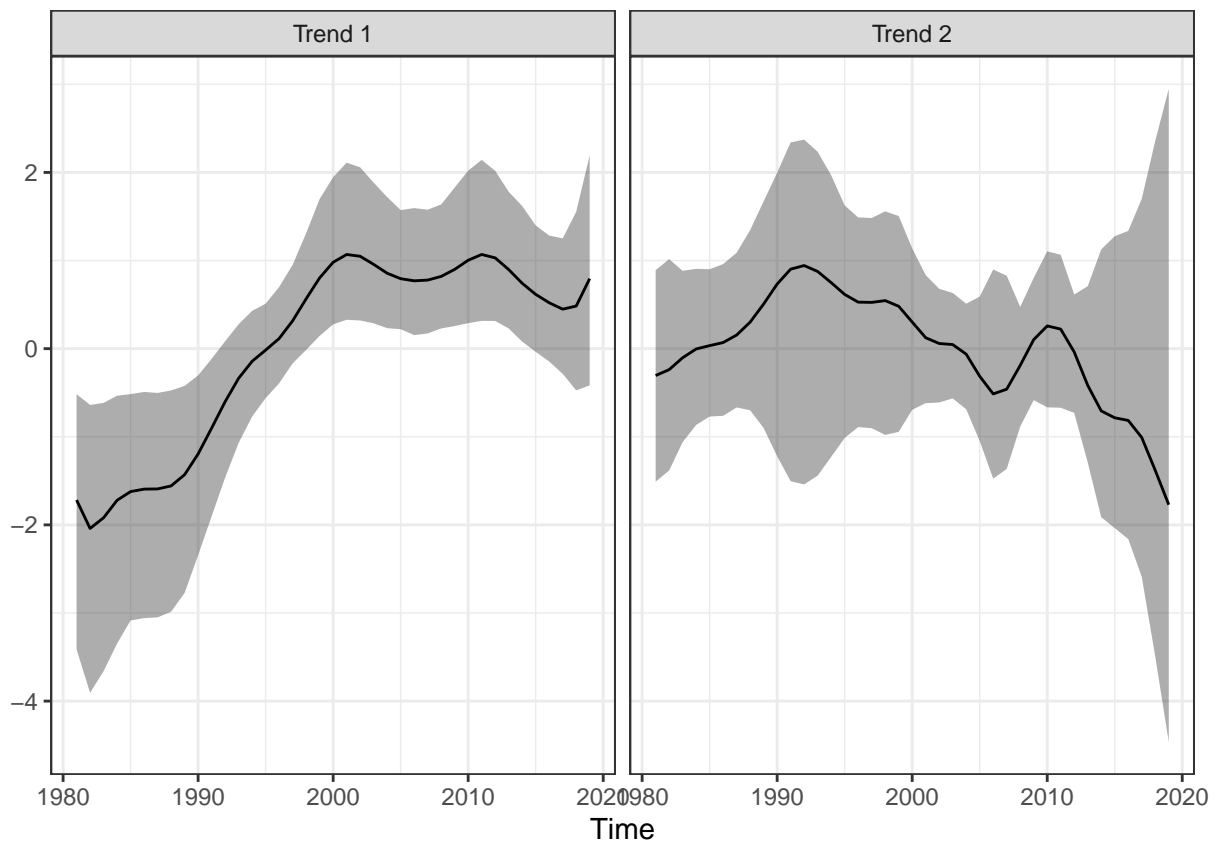


Figure 2: Figure 02

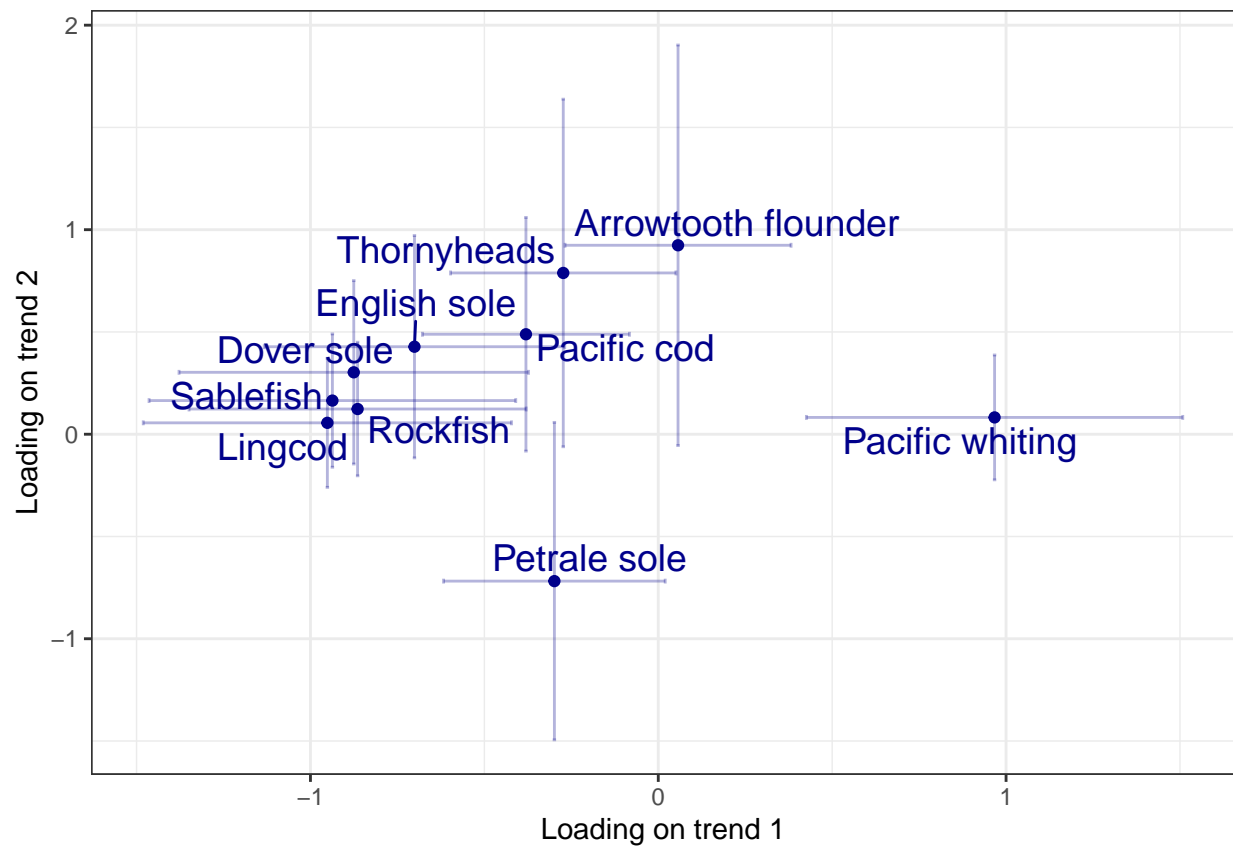


Figure 3: Figure 03

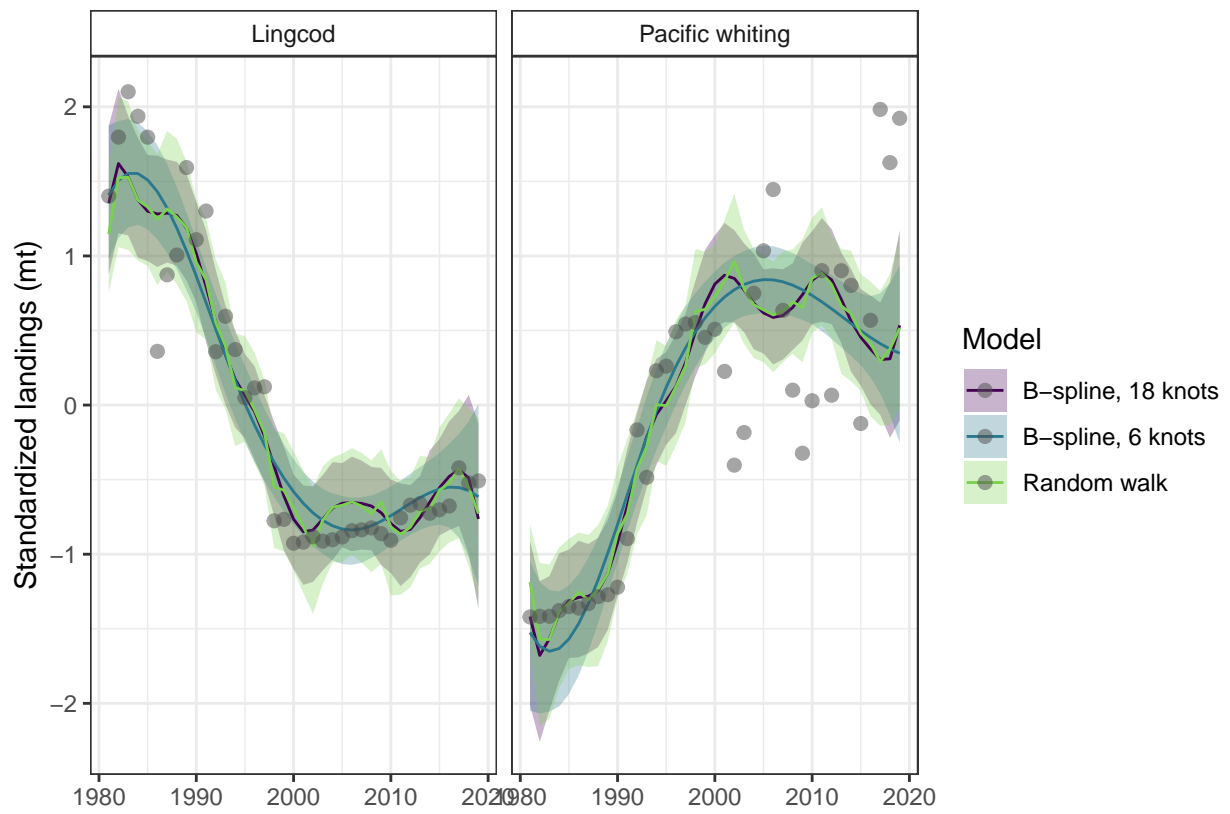


Figure 4: Figure 04

References

- Anderson, S. C., and E. J. Ward. 2019. Black swans in space: Modeling spatiotemporal processes with extremes. *Ecology* 100:e02403.
- Auger-Méthé, M., K. Newman, D. Cole, F. Empacher, R. Gryba, A. A. King, V. Leos-Barajas, J. M. Flemming, A. Nielsen, G. Petris, and L. Thomas. 2020. A guide to state-space modeling of ecological time series. *arXiv:2002.02001* [q-bio, stat].
- Bograd, S. J., D. A. Checkley, and W. S. Wooster. 2003. CalCOFI: A half century of physical, chemical, and biological research in the California Current System. *Deep Sea Research Part II: Topical Studies in Oceanography* 50:2349–2353.
- Bürkner, P.-C., J. Gabry, and A. Vehtari. 2020. Approximate leave-future-out cross-validation for Bayesian time series models. *Journal of Statistical Computation and Simulation* 90:2499–2523.
- Carpenter, B., A. Gelman, M. D. Hoffman, D. Lee, B. Goodrich, M. Betancourt, M. Brubaker, J. Guo, P. Li, and A. Riddell. 2017. *Stan*: A Probabilistic Programming Language. *Journal of Statistical Software* 76.
- Chamberlain, S. 2020. Rerddap: General purpose client for 'ERDDAP' servers. *manual*.
- Cherif, A., H. Cardot, and R. Boné. 2011. SOM time series clustering and prediction with recurrent neural networks. *Neurocomputing* 74:1936–1944.
- Clark, J. S., and O. N. Bjørnstad. 2004. Population Time Series: Process Variability, Observation Errors, Missing Values, Lags, and Hidden States. *Ecology* 85:3140–3150.
- Dennis, B., J. M. Ponciano, S. R. Lele, M. L. Taper, and D. F. Staples. 2006. Estimating Density Dependence, Process Noise, and Observation Error. *Ecological Monographs* 76:323–341.
- Gelman, A., and D. B. Rubin. 1992. Inference from Iterative Simulation Using Multiple Sequences. *Statistical Science* 7:457–472.
- Harvey, C., N. Garfield, G. Williams, N. Tolimieri, I. Schroeder, E. Hazen, K. Andrews, K. Barnas, S. Bograd, R. Brodeur, B. Burke, J. Cope, L. deWitt, J. Field, J. Fisher, T. Good, C. Greene, D. Holland, M. Hunsicker, and S. Zador. 2018. Ecosystem Status Report of the California Current for 2018: A Summary of Ecosystem Indicators Compiled by the California Current Integrated Ecosystem Assessment Team (CCIEA).
- Hastie, T. J. 1992. Statistical Models in S. *in* J. M. Chambers and T. J. Hastie, editors. Wadsworth

308 & Brooks/Cole.

309 Hoffman, M. D., and A. Gelman. 2014. The No-U-Turn Sampler: Adaptively Setting Path Lengths in
310 Hamiltonian Monte Carlo. *Journal of Machine Learning Research* 15:1593–1623.

311 Holan, S. H., and N. Ravishanker. 2018. Time series clustering and classification via frequency domain
312 methods. *WIREs Computational Statistics* 10:e1444.

313 Holmes, E. E., E. J. Ward, and M. D. Scheuerell. 2020. Analysis of multivariate time-series using the
314 MARSS package. NOAA Fisheries, Northwest Fisheries Science Center, 2725 Montlake Blvd E., Seattle,
315 WA 98112.

316 Holmes, E. E., E. J. Ward, and K. Wills. 2012. MARSS: Multivariate autoregressive state-space models
317 for analyzing time-series data. *R Journal* 4:11–19.

318 Hovel, R., S. Carlson, and T. Quinn. 2016. Climate change alters the reproductive phenology and
319 investment of a lacustrine fish, the three-spine stickleback. *Global Change Biology* 23.

320 Kimeldorf, G. S., and G. Wahba. 1970. A Correspondence Between Bayesian Estimation on Stochastic
321 Processes and Smoothing by Splines. *The Annals of Mathematical Statistics* 41:495–502.

322 Knape, J. 2008. Estimability of Density Dependence in Models of Time Series Data. *Ecology* 89:2994–
323 3000.

324 Latimer, A. M., S. Banerjee, H. S. Jr, E. S. Mosher, and J. A. S. Jr. 2009. Hierarchical models facilitate
325 spatial analysis of large data sets: A case study on invasive plant species in the northeastern United States.
326 *Ecology Letters* 12:144–154.

327 Liao, T. W. 2005. Clustering of time series data—a survey. *Pattern Recognition* 38:1857–1874.

328 MacCall, A. D. 2003. Status of Bocaccio off California in 2003. In Appendix to the status of the Pacific
329 coast groundfish fishery through 2003: Stock assessment and fishery evaluation. Pacific Fishery Management
330 Council, Portland, OR.

331 McClatchie, S., R. Goericke, J. Koslow, F. Schwing, S. Bograd, R. Charter, W. Watson, N. Lo, K.
332 Hill, J. Gottschalck, M. L’Heureux, Y. Xue, W. Peterson, R. Emmett, C. Collins, G. Gaxiola-Castro, R.
333 Durazo, M. Kahru, B. Mitchell, and E. Bjorkstedt. 2008. The state of the California Current, 2007-2008: La
334 Niña conditions and their effects on the ecosystem. California Cooperative Oceanic Fisheries Investigations
335 Reports 49:39–76.

336 Mosek, H., L. Charter, W. Watson, I. Ambrose, N. Shakon, K. Charter, E. Saniiknoi, S. Fisheies,

S. Center, M. Fi, and H. Service. 2000. Abundance and distribution of rockfish (*Sebastes*) larvae in the Southern California Bight in relation to environmental conditions and fishery exploitation. ABUNDANCE AND DISTRIBUTION OF ROCKFISH LARVAE CalCOFI Rep 41.

Moser, H. G., R. L. Charter, W. Watson, A. Amurose, P. E. Smith, E. M. Sani, and S. R. Charter. 2001. The CalCOFI Ichthyoplankton time series: Potential contributions to the management of rocky-shore fishes 42:17.

Patterson, T. A., L. Thomas, C. Wilcox, O. Ovaskainen, and J. Matthiopoulos. 2008. State-space models of individual animal movement. *Trends in Ecology & Evolution* 23:87–94.

Pedersen, E. J., D. L. Miller, G. L. Simpson, and N. Ross. 2019. Hierarchical generalized additive models in ecology: An introduction with mgcv. *PeerJ* 7:e6876.

PFMC. 2020. Status of the Pacific Coast Groundfish Fishery: Stock Assessment and Fishery Evaluation. The Pacific Fishery Management Council, Portland, OR.

R Core Team. 2020. R: A language and environment for statistical computing. manual, Vienna, Austria.

Roberts, S., M. Osborne, M. Ebdon, S. Reece, N. Gibson, and S. Aigrain. 2013. Gaussian processes for time-series modelling. *Philosophical Transactions of the Royal Society A: Mathematical, Physical and Engineering Sciences* 371:20110550.

Sardá-Espinosa, A. 2019. Time-Series Clustering in R Using the dtwclust Package. *The R Journal* 11:22–43.

Stan Development Team. 2016. RStan: The R interface to Stan.

Vehtari, A., J. Gabry, M. Magnusson, Y. Yao, P.-C. Bürkner, T. Paananen, and A. Gelman. 2020. Loo: Efficient leave-one-out cross-validation and WAIC for Bayesian models.

Vehtari, A., A. Gelman, and J. Gabry. 2017. Practical Bayesian model evaluation using leave-one-out cross-validation and WAIC. *Statistics and Computing* 27:1413–1432.

Ward, E. J., S. Anderson C., L. Damiano A., M. Hunsicker E., and M. Litzow A. 2019. Modeling regimes with extremes: The bayesdfa package for identifying and forecasting common trends and anomalies in multivariate time-series data. *The R Journal* 11:46.

Ward, E. J., H. Chirakkal, M. González-Suárez, D. Auriolles-Gamboa, E. E. Holmes, and L. Gerber. 2010. Inferring spatial structure from time-series data: Using multivariate state-space models to detect

366 metapopulation structure of California sea lions in the Gulf of California, Mexico. *Journal of Applied*
367 *Ecology* 47:47–56.

368 Warlick, A., E. Steiner, and M. Guldin. 2018. History of the West Coast groundfish trawl fishery
369 Tracking socioeconomic characteristics across different management policies in a multispecies fishery. *Marine*
370 *Policy* 93:9–21.

371 Wood, S. N. 2011. Fast stable restricted maximum likelihood and marginal likelihood estimation of
372 semiparametric generalized linear models. *Journal of the Royal Statistical Society: Series B (Statistical*
373 *Methodology)* 73:3–36.

374 Zuur, A. F., R. J. Fryer, I. T. Jolliffe, R. Dekker, and J. J. Beukema. 2003a. Estimating common
375 trends in multivariate time series using dynamic factor analysis. *Environmetrics* 14:665–685.

376 Zuur, A. F., I. D. Tuck, and N. Bailey. 2003b. Dynamic factor analysis to estimate common trends in
377 fisheries time series. *Canadian Journal of Fisheries and Aquatic Sciences* 60:542–552.